Low-Frequency Electromagnetic Waves on a Twisted-Pair Transmission Line

Kirk T. McDonald

Joseph Henry Laboratories, Princeton University, Princeton, NJ 08544

(December 24, 2008)

1 Problem

Discuss the electromagnetic waves that can propagate in the space around a transmission line whose form is a double helix of radius a and longitudinal period $p \approx a$. The pitch angle ψ of the helical windings with respect to the transverse planes is given by,

$$\cot\psi = k_p a = \frac{2\pi a}{p}\,. \tag{1}$$

The angle θ of the windings with respect to the axis of the line is then $\theta = \pi/2 - \psi$, *i.e.*,

$$\tan\theta = k_p a. \tag{2}$$

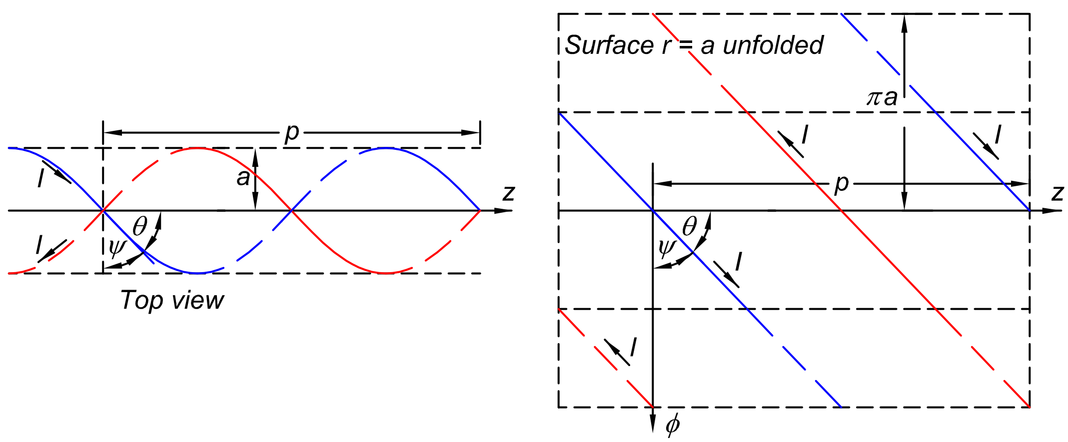

Such lines are extensively used for telephone communication at low frequencies for which $ka, kp \ll 1$, where $k = 2\pi/\lambda = \omega/v$ is the wave number at angular frequency ω, and v is the wave velocity. For the case that $ka, kp \gg 1$ the waves can be thought of following the helical conductors such that the group velocity along the axis of the helix is,

$$v_{g,z} \approx c\cos\theta. \tag{3}$$

Show that even at low frequencies eq. (3) is a reasonable approximation when $a \approx p$, but when $a \ll p$ (a gentle twist) then $v_{g,z} \approx c\sqrt{\cos\theta}$.

2 Solution

Despite the common use of twisted-pair transmission lines, this problem seems little discussed in the literature. In the case of two-dimensional conductors there exist transverse electromagnetic (TEM) waves of the form $e^{i(kz-\omega t)}$ times the (transverse) static electric and magnetic field patterns. However, TEM waves will not propagate along a twisted pair of wires, whose structure is three-dimensional.

Waves on a single helical conductor have been discussed in the context of traveling-wave amplifiers in the "sheath" approximation [1, 2], where only the part of the waves that are independent of azimuth are analyzed. A fairly general discussions of waves on twisted-pair conductors for $ka \approx kp \approx 1$ has been given in [3], again in the context of traveling-wave amplifiers.[1,2]

Here, we emphasize the low-frequency behavior, when $ka, kp \ll 1$.

2.1 General Form of the Fields in Cylindrical Coordinates

We use a cylindrical coordinate system (r, ϕ, z) whose axis is that of the transmission line. We ignore the insulation typically found on the wires of a twisted-pair line, and assume that the space outside the wires is vacuum.

The electromagnetic fields $\mathbf{E}$ and $\mathbf{B}$ with time dependence $e^{-i\omega t}$ satisfy the vector Helmholtz equation,

$$(\nabla^2 + k_f^2)\mathbf{E}, \mathbf{B} = 0, \tag{4}$$

outside the wires, where,

$$k_f = \frac{\omega}{c} = \frac{2\pi}{\lambda_f}\,. \tag{5}$$

However, in cylindrical coordinates only their z-components satisfy the scalar Helmholtz equation,[3]

$$(\nabla^2 + k_f^2)E_z, B_z = 0. \tag{6}$$

We look for wavefunctions for E_z and B_z that propagate in the z-direction with the form,

$$f_m(r)\, e^{-im\phi}\, e^{i(k_m z-\omega t)}, \tag{7}$$

where m is an integer. The (right-handed) helical conductor rotates by $\phi = k_p z = 2\pi z/p$ as z increases, so we expect the wavefunction (7) to include this symmetry via a phase factor $e^{-im(\phi - k_p z)}$ such that the waveform rotates as it advances. The z-dependent part of this phase contributes to the wave number k_m, which takes the form,[4]

$$k_m = k_0(\omega) + mk_p. \tag{8}$$

[1] See [4] for the case of cross-wound helices.

[2] The magnetic fields of twisted pairs have been discussed in [5, 6, 7, 8]. Twisted-pair structures with large currents are used as undulators to generate energetic photon beams at particle accelerators (see, for example, [9]).

[3] See, for example, p. 116 of [10] or Appendix A, p. 6 of [11].

[4] The present case contrasts with that of so-called Bessel beams of order m (see, for example, the Appendix of [12]) where the drive currents are limited to a small region in z, rather than being periodic in z, such that $k_m = k_0$ for any index m.

We are mainly interested in waves that propagate in the $+z$ direction, for which the index m must be non-negative at low frequencies where $0 < k_0 \ll k_p$.[5]

The phase φ_m of the wave function (7) is $\varphi_m = \mathbf{k}^{(m)} \cdot \mathbf{x} - \omega t = k_m z - m\phi - \omega t$, where the wave vector $\mathbf{k}^{(m)}$ is given by,

$$\mathbf{k}^{(m)} = \boldsymbol{\nabla}\varphi_m = k_m\,\hat{\mathbf{z}} - \frac{m}{r}\,\hat{\boldsymbol{\phi}}. \tag{9}$$

The phase velocity $v_{p,m}$ of a partial wave of index m is,

$$\mathbf{v}_{p,m} = \frac{\omega}{k^{(m)}}\,\hat{\mathbf{k}}^{(m)} = \frac{ck_f}{k_m^2 + m^2/r^2}\left(k_m\,\hat{\mathbf{z}} - \frac{m}{r}\,\hat{\boldsymbol{\phi}}\right). \tag{10}$$

We expect that $k_0 \lesssim k_f$ ($\ll k_p$) so that $\mathbf{v}_{p,0} \lesssim c\,\hat{\mathbf{z}}$, but for nonzero index m we have that $k_m \approx m k_p$, and hence,

$$\mathbf{v}_{p,m} \approx \frac{ck_f\,r}{m[1 + (k_p\,r)^2]}\left(k_p\,r\,\hat{\mathbf{z}} - \hat{\boldsymbol{\phi}}\right), \tag{11}$$

which is small compared to c at any value of r. The wave vector $\mathbf{k}^{(m)}$ (and the phase velocity $\mathbf{v}_{p,m}$) make angle θ_k to the z-axis given by,

$$\tan\theta_k = -\frac{1}{k_p\,r} \tag{12}$$

for any nonzero index m. Note that at $r = a$ the wave vector is at right angles to the direction of the helical windings, for which $\tan\theta = k_p a$.

The group velocity of a partial wave is,[6]

$$\mathbf{v}_{g,m} = \boldsymbol{\nabla}_{\mathbf{k}^{(m)}} = \frac{\partial\omega}{\partial\mathbf{k}^{(m)}}, \tag{13}$$

whose only nonzero component is,

$$v_{g,m,z} = \frac{d\omega}{dk_z^{(m)}} = \frac{d\omega}{dk_m} \approx \frac{1}{dk_m/d\omega} = \frac{1}{dk_0/d\omega} = v_{g,0,z} \equiv v_{g,z}, \tag{14}$$

independent of index m. We expect that $v_{g,z} \lesssim c$ in the low-frequency limit.

Using eqs. (7)-(8) in the Helmholtz equation (6), we see that the radial function f_m obeys the Bessel equation,

$$\frac{1}{r}\frac{d}{dr}\left(r\frac{df_m}{dr}\right) - \left(k_m^2 - k_f^2 + \frac{m^2}{r^2}\right)f = 0, \tag{15}$$

where $|k_m| \geq k_0 > k_f$. The solutions to eq. (15) should remain finite at $r = 0$ and ∞, so for $r < a$ we use the modified Bessel function $I_m(k'_m r)$, and for $r > a$ we use $K_m(k'_m r)$, where,

$$k'_m = \sqrt{k_m^2 - k_f^2}. \tag{16}$$

[5]Waves with index m negative (both for single helix and double-helix configurations) have their phase and group velocities in opposite directions. An application of such waves is the backward wave oscillator. See, for example, [13].

[6]See, for example, sec. 2.1 of [15].

That is, the longitudinal components of the electric and magnetic fields outside the wires have the forms,

$$E_z(r<a) = \sum_m E_m \frac{I_m(k'_m r)}{I_m(k'_m a)} e^{-im\phi}\, e^{i(k_m z-\omega t)}, \quad E_z(r>a) = \sum_m E_m \frac{K_m(k'_m r)}{K_m(k'_m a)} e^{-im\phi}\, e^{i(k_m z-\omega t)}, \tag{17}$$

$$B_z(r<a) = \sum_m B_m \frac{I_m(k'_m r)}{I'_m(k'_m a)} e^{-im\phi}\, e^{i(k_m z-\omega t)}, \quad B_z(r>a) = \sum_m B_m \frac{K_m(k'_m r)}{K'_m(k'_m a)} e^{-im\phi}\, e^{i(k_m z-\omega t)}, \tag{18}$$

where B_m and E_m are constants to be determined, and $I'_m(k'_m a) = dI_m(k'_m a)/dr$. In eq. (17) we have noted that the Maxwell equation $\boldsymbol{\nabla}\times\mathbf{E} = ik_f\mathbf{B}$ (in Gaussian units) implies that E_z (and E_ϕ) is continuous across the surface $r = a$. We verify later that the normalization of coefficients B_m to $I'_m(k'_m a)$ and $K'_m(k'_m a)$ insures continuity of the magnetic field component B_r across this surface, as required by the Maxwell equation $\boldsymbol{\nabla}\cdot\mathbf{B} = 0$.

The waves are driven by the current density $\mathbf{J}$ in the twisted pair, which we can write as,

$$\mathbf{J}(\mathbf{x}, t) = J(\phi, z, t)\delta(r-a)(\sin\theta\,\hat{\boldsymbol{\phi}} + \cos\theta\,\hat{\mathbf{z}}), \tag{19}$$

which points along the local direction of the twisted-pair conductors, and is confined to a thin cylinder of radius a. The wavefunction $J(\phi, z, t)$ must have the same dependence on ϕ, z and t as eqs. (17)-(18), namely,

$$J(\phi, z, t) = \sum_m J_m\, e^{-im\phi}\, e^{i(k_m z-\omega t)}, \tag{20}$$

assuming that the current only flows in the direction of the helical windings.

For a twisted pair, the current at fixed z and azimuth $\phi+\pi$ is opposite to that at azimuth ϕ, which implies that J_m is nonzero only for odd m

In the case of a pair of wires of small diameter, the expansion (20) has contributions from all odd integers m. We will make a simplifying assumption that only the term $m = 1$ is important, which corresponds to replacing the helical wires by a pair of helical wire bundles, each of which extends over $\Delta\phi = \pi$, such that the current in the bundles at fixed z varies as $\cos\phi$. If the peak current in each wire is I, then,

$$J(\phi, z, t) = \frac{I}{2a\cos\theta}\, e^{-i\phi}\, e^{i(k_1 z-\omega t)}, \tag{21}$$

$$E_z(r<a) = E_1 \frac{I_1(k'_1 r)}{I_1(k'_1 a)} e^{-i\phi} e^{i(k_1 z-\omega t)}, \quad E_z(r>a) = E_1 \frac{K_1(k'_1 r)}{K_1(k'_1 a)} e^{-i\phi} e^{i(k_1 z-\omega t)}, \tag{22}$$

and

$$B_z(r<a) = B_1 \frac{I_1(k'_1 r)}{I'_1(k'_1 a)}\, e^{-i\phi}\, e^{i(k_1 z-\omega t)}, \quad B_z(r>a) = B_1 \frac{K_1(k'_1 r)}{K'_1(k'_1 a)}\, e^{-i\phi}\, e^{i(k_1 z-\omega t)}. \tag{23}$$

To deduce the other field components from the forms (17)-(18) it is useful to note that the electromagnetic fields can also be derived from from electric and magnetic Hertz vectors $\mathbf{Z}_E$ and $\mathbf{Z}_M$ (also called polarization potentials; see, for example, sec. 1.11 and chap. 6 of [16]), each of which has only a z-component. These Hertz scalars, which we call Z_E and Z_M, obey the scalar Helmholtz equation, $(\nabla^2 + k_f^2) Z_E, Z_M = 0$, outside the wires. Thus, the Hertz scalars also have the forms (22)-(23), and we will verify that,

$$Z_E = -\frac{E_z}{{k'_1}^2}, \qquad Z_M = -\frac{B_z}{{k'_1}^2}. \tag{24}$$

The scalar and vector potentials V and $\mathbf{A}$ are related to the Hertz vectors according to,

$$V = -\boldsymbol{\nabla} \cdot \mathbf{Z}_E, \qquad \mathbf{A} = \frac{1}{c}\frac{\partial \mathbf{Z}_E}{\partial t} + \boldsymbol{\nabla} \times \mathbf{Z}_M, \tag{25}$$

and hence the electric and magnetic fields $\mathbf{E}$ and $\mathbf{H}$ are given by,

$$\mathbf{E} = \boldsymbol{\nabla}(\boldsymbol{\nabla} \cdot \mathbf{Z}_E) - \frac{1}{c^2}\frac{\partial^2 \mathbf{Z}_E}{\partial t^2} - \frac{1}{c}\boldsymbol{\nabla} \times \frac{\partial \mathbf{Z}_M}{\partial t}, \qquad \mathbf{B} = \frac{1}{c}\boldsymbol{\nabla} \times \frac{\partial \mathbf{Z}_E}{\partial t} + \boldsymbol{\nabla} \times (\boldsymbol{\nabla} \times \mathbf{Z}_M). \tag{26}$$

The components of the electromagnetic fields in cylindrical coordinates in terms of the Hertz scalars Z_E and Z_M are (see sec. 6.1 of [16] with $u^1 = r$, $u^2 = \phi$, $h_1 = 1$ and $h_2 = r$),

$$E_r = \frac{\partial^2 Z_E}{\partial r \partial z} - \frac{1}{cr}\frac{\partial^2 Z_M}{\partial \phi \partial t}, \tag{27}$$

$$E_\phi = \frac{1}{r}\frac{\partial^2 Z_E}{\partial \phi \partial z} + \frac{1}{c}\frac{\partial^2 Z_M}{\partial r \partial t}, \tag{28}$$

$$E_z = -\frac{1}{r}\left[\frac{\partial}{\partial r}\left(r\frac{\partial Z_E}{\partial r}\right) + \frac{\partial}{\partial \phi}\left(\frac{1}{r}\frac{\partial Z_E}{\partial \phi}\right)\right], \tag{29}$$

$$B_r = \frac{\partial^2 Z_M}{\partial r \partial z} + \frac{1}{cr}\frac{\partial^2 Z_E}{\partial \phi \partial t}, \tag{30}$$

$$B_\phi = \frac{1}{r}\frac{\partial^2 Z_M}{\partial \phi \partial z} - \frac{1}{c}\frac{\partial^2 Z_E}{\partial r \partial t}, \tag{31}$$

$$B_z = -\frac{1}{r}\left[\frac{\partial}{\partial r}\left(r\frac{\partial Z_M}{\partial r}\right) + \frac{\partial}{\partial \phi}\left(\frac{1}{r}\frac{\partial Z_M}{\partial \phi}\right)\right]. \tag{32}$$

For what it's worth, the fields associated with Z_E are transverse magnetic *(TM), while those associated with Z_M are* transverse electric *(TE).*

To use the forms (22)-(23) in eqs. (27)-(32), we note that,

$$I'_m(k'_m r) = k'_m I_{m-1} - \frac{m I_m}{r} = k'_m I_{m+1} + \frac{m I_m}{r}, \qquad \frac{1}{r}\frac{d[r I'_m(k'_m r)]}{dr} = \left({k'_m}^2 + \frac{m^2}{r}\right) I_m, \tag{33}$$

$$K'_m(k'_m r) = -k'_m K_{m-1} - \frac{m K_m}{r} = -k'_m K_{m+1} + \frac{m K_m}{r}, \quad \frac{1}{r}\frac{d[r K'_m(k'_m r)]}{dr} = \left({k'_m}^2 + \frac{m^2}{r}\right) K_m, \tag{34}$$

so that for $r < a$ the field components are,

$$E_r = -\frac{1}{{k'_1}^2}\left[ik_1 E_1 \frac{I'_1(k'_1 r)}{I_1(k'_1 a)} + \frac{k_f}{r} B_1 \frac{I_1(k'_1 r)}{I'_1(k'_1 a)}\right] e^{-i\phi}\, e^{i(k_1 z - \omega t)}, \tag{35}$$

$$E_\phi = -\frac{1}{{k'_1}^2}\left[\frac{k_1}{r}E_1\frac{I_1(k'_1 r)}{I_1(k'_1 a)} - ik_f B_1 \frac{I'_1(k'_1 r)}{I'_1(k'_1 a)}\right] e^{-i\phi}\, e^{i(k_1 z - \omega t)}, \tag{36}$$

$$E_z = -{k'_1}^2 Z_E = E_1 \frac{I_1(k'_1 r)}{I_1(k'_1 a)} e^{-i\phi}\, e^{i(k_1 z - \omega t)}, \tag{37}$$

$$B_r = \frac{1}{{k'_1}^2}\left[\frac{k_f}{r}E_1\frac{I_1(k'_1 r)}{I_1(k'_1 a)} - ik_1 B_1 \frac{I'_1(k'_1 r)}{I'_1(k'_1 a)}\right] e^{-i\phi}\, e^{i(k_1 z - \omega t)}, \tag{38}$$

$$B_\phi = -\frac{1}{{k'_1}^2}\left[ik_f E_1\frac{I'_1(k'_1 r)}{I_1(k'_1 a)} + \frac{k_1}{r} B_1 \frac{I_1(k'_1 r)}{I'_1(k'_1 a)}\right] e^{-i\phi}\, e^{i(k_1 z - \omega t)}, \tag{39}$$

$$B_z = -{k'_1}^2 Z_M = B_1 \frac{I_1(k'_1 r)}{I'_1(k'_1 a)} e^{-i\phi}\, e^{i(k_1 z - \omega t)}, \tag{40}$$

and for $r > a$ we have the forms (35)-(40) with the substitution $I_1 \to K_1$.

We now see that the continuity of E_ϕ and B_r across the surface $r = a$, as previously mentioned, is satisfied by the above forms.

2.2 Determination of k_0 and the Group and Signal Velocities

The current in the helical windings is assumed to flow only at angle θ with respect to the z-axis, so that for good conductors the conductivity of the "wires" is "infinite" in this direction, and zero in the perpendicular directions. Hence, the electric field on the surface of the cylinder $r = a$ must be perpendicular to the direction of the current, *i.e.*,

$$E_\phi(r = a) = -\cot\theta E_z(r = a), \tag{41}$$

and hence,

$$\left({k'_1}^2 a\cot\theta - k_1\right) E_1 + ik_f a B_1 = 0. \tag{42}$$

Also, the tangential component of the magnetic field in the direction of the current must be continuous at $r = a$, which implies that,

$$B_z(r = a_-) + \tan\theta B_\phi(r = a_-) = B_z(r = a_+) + \tan\theta B_\phi(r = a_+), \tag{43}$$

and hence,

$$ik_f a I'_1(k'_1 a) K'_1(k'_1 a) E_1 + \left({k'_1}^2 a\cot\theta - k_1\right) I_1(k'_1 a) K_1(k'_1 a) B_1 = 0. \tag{44}$$

For the simultaneous linear equations (42) and (44) to be consistent, the determinant of the coefficient matrix must vanish, *i.e.*,

$$\left({k'_1}^2 a\cot\theta - k_1\right)^2 = -(k_f a)^2 \frac{I'_1(k'_1 a) K'_1(k'_1 a)}{I_1(k'_1 a) K_1(k'_1 a)}\,. \tag{45}$$

This determines k_0 (and therefore k_1 and k'_1) in terms of a, p and k_f.

We restrict our attention to low frequencies such that $k_f a \ll 1$. *In the limit that k_f and k_0 vanish, then $k_1 = k'_1 = k_p$ and $k_p^2 a\cot\theta - k_p = 0$, recalling that $\cot\theta = 1/k_p a$, so that eq. (45) is satisfied.* For small k_f and k_0 we approximate,

$$k_1 = k_p + k_0 \approx k_p\left(1 + \frac{k_0}{k_p}\right), \qquad {k'_1}^2 = k_1^2 - k_f^2 \approx k_p^2\left(1 + 2\frac{k_0}{k_p} - \frac{k_f^2}{k_p^2}\right), \tag{46}$$

so that it suffices to take the arguments of the Bessel functions as $k_p a$. Using these in eq. (45) and recalling eqs. (33)-(34), we find,

$$\left(k_0 - \frac{k_f^2}{k_p}\right)^2 \approx k_0^2 \approx -(k_f a)^2 \frac{I_1'(k_p a) K_1'(k_p a)}{I_1(k_p a) K_1(k_p a)} = k_f^2 C^2(k_p a), \tag{47}$$

where the constant C defined by,

$$C^2(k_p a) = -a^2 \frac{I_1'(k_p a) K_1'(k_p a)}{I_1(k_p a) K_1(k_p a)} = \frac{[k_p a I_0(k_p a) - I_1(k_p a)][k_p a K_0(k_p a) + K_1(k_p a)]}{I_1(k_p a) K_1(k_p a)} \tag{48}$$

is real and positive since K_1' is negative, as seen in the figure below, from p. 374 of [14].

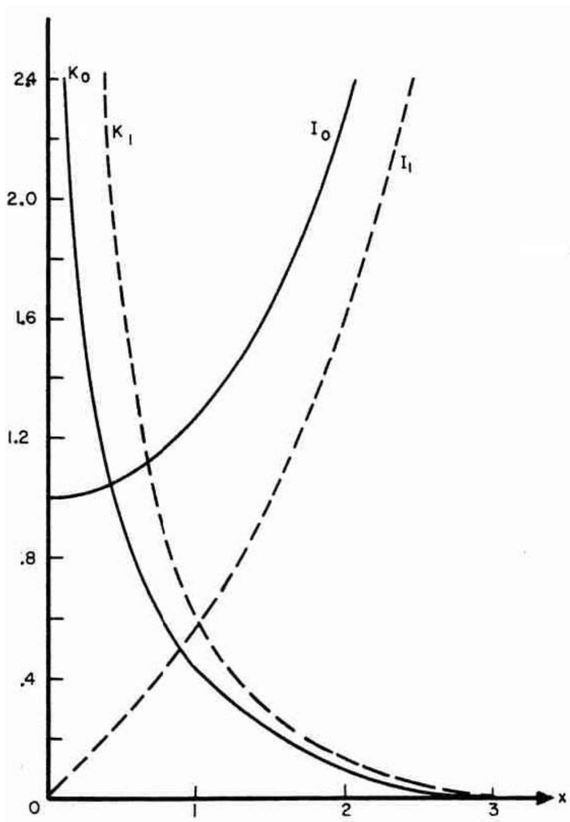

For example, if $\theta = 45°$ then $k_p a = 1$, and,

$$C^2(1) \approx \frac{[1.2 - 0.55][0.4 + 0.6]}{0.55 \cdot 0.6} \approx 2, \tag{49}$$

and $C(1) \approx 1.4$.

For $k_p a \ll 1$ (gentle twist) then $I_0(k_p a) \approx 1 + (k_p a)^2/2$, $I_1(k_p a) \approx k_p a/2 + (k_p a)^3/8$, and $K_1(k_p a) \gg k_p a K_0(k_p a)$, so we have,

$$C^2(k_p a \ll 1) \approx \frac{k_p a I_0(k_p a)}{I_1(k_p a)} - 1 \approx 1 + (k_p a)^2/2 \approx \frac{1}{\cos\theta}\,. \tag{50}$$

From eq. (47), the wave number k_0 is,

$$k_0 \approx C k_f = C \frac{\omega}{c}\,. \tag{51}$$

Recalling from eqs. (8)-(9) that $\mathbf{k}^{(1)} \equiv \mathbf{k} = (k_0 + k_p)\,\hat{\mathbf{z}} - \hat{\boldsymbol{\phi}}/r$, eq. (51) can be recast as the dispersion relation,

$$\omega = \omega(\mathbf{k}^{(1)}) \equiv \omega(\mathbf{k}) \approx \frac{c}{C} k_0 = \frac{c}{C}\left(k_z - \frac{k_p r}{r}\right) = \frac{c}{C}(k_z + k_p r k_\phi). \tag{52}$$

Then, the group velocity vector (13) is,[7]

$$\mathbf{v}_g = \boldsymbol{\nabla}_{\mathbf{k}}\omega(\mathbf{k}) = \frac{\partial \omega}{\partial k_z}\,\hat{\mathbf{z}} + \frac{\partial \omega}{\partial k_\phi}\,\hat{\boldsymbol{\phi}} \approx \frac{c}{C}(\hat{\mathbf{z}} + k_p r\,\hat{\boldsymbol{\phi}}). \tag{53}$$

While the z-component, $v_{g,z}$ of the group velocity is independent of radius r, the group velocity vector $\mathbf{v}_g$ makes angle θ_g to the z-axis given by,

$$\tan\theta_g \approx k_p r. \tag{54}$$

At very small r the group velocity is essentially parallel to the z-axis, but at large r lines of the group velocity form helices with very small pitch. The magnitude of the group velocity is,

$$v_g \approx \frac{c}{C}\sqrt{1 + (k_p r)^2}, \tag{55}$$

which exceeds c at large r. However, the signal velocity v_s is clearly,

$$v_s = v_{g,z} = \frac{c}{C} < c. \tag{56}$$

Comparing with eq. (12), we see that the group velocity $\mathbf{v}_g$ is perpendicular to the phase velocity $\mathbf{v}_p$, and that on the surface $r = a$ the group velocity is along the direction of the helical windings.

For $\theta = 45^\circ$ we find that $v_{g,z} \approx c/C \approx 0.7c \approx c\cos\theta$ for an uninsulated twisted-pair transmission line. This happens to be close to the group velocity of typical insulated, untwisted two-wire transmission lines!

For gently twisted, uninsulated pairs and low frequencies, eqs. (50) and (53) indicate that $v_{g,z} \approx c\sqrt{\cos\theta}$.

2.3 Characteristic Impedance Z_0 at Low Frequencies

To evaluate the characteristic impedance of the transmission line at low frequencies, we,consider the radial electric field (35) for $r < a$, for which we need to know the constants B_1 and E_1 in terms of the (peak) current I in the windings.

We can relate B_1 to the (peak) current I in the twisted pair via Ampère's law for a small loop of length dz in the r-z plane that surrounds a short segment of the conductor where the current is maximal,

$$\begin{aligned} \frac{4\pi}{c} I_{\text{max, through loop}} = \frac{4\pi}{c}\frac{\pi}{p} I \quad &= \quad |B_z(r = a_-) - B_z(r = a+)|\,dz \\ &\approx \quad B_1\left(\frac{I_1(k_p a)}{I_1'(k_p a)} - \frac{K_1(k_p a)}{K_1'(k_p a)}\right) dz. \end{aligned} \tag{57}$$

[7] The group velocity vector follows straight lines in homogenous media (see, for example, sec. 2.1 of [15]). Because of the twisted conductors, the present problem is not one of a homogenous medium, and the group velocity vector field need not have straight streamlines.

That is,

$$B_1 = \frac{4\pi}{c} \frac{\pi}{p} \frac{-I_1'(k_p a)K_1'(k_p a)}{I_1'(k_p a)K_1(k_p a) - I_1(k_p a)K_1'(k_p a)} I = \frac{4\pi}{c} \frac{k_p}{2a} C^2 D I, \tag{58}$$

where,

$$\begin{aligned} D(k_p a) &= \frac{1}{a} \frac{I_1(k_p a)K_1(k_p a)}{I_1'(k_p a)K_1(k_p a) - I_1(k_p a)K_1'(k_p a)} \\ &= \frac{I_1(k_p a)K_1(k_p a)}{[k_p a I_0(k_p a) - I_1(k_p a)]K_1(k_p a) + I_1(k_p a)[k_p a K_0(k_p a) + K_1(k_p a)]} . \end{aligned} \tag{59}$$

Then, eqs. (42) and (51) tell us that,

$$E_1 \approx -\frac{i k_f a}{k_0} B_1 \approx -\frac{ia}{C} B_1 = -\frac{4\pi}{c} \frac{i k_p}{2} C D I. \tag{60}$$

From eq. (35) we see that the radial electric field for $r < a$ is largely due to the term in E_1 since $k_f \ll k_1$ (at low frequencies). That is,

$$E_r(r < a) \approx -\frac{i}{k_p} E_1 \frac{I_1'(k_p r)}{I_1(k_p a)} e^{-i\phi} e^{i(k_1 z - \omega t)} = -\frac{4\pi}{c} \frac{CDI}{2} \frac{I_1'(k_p r)}{I_1(k_p a)} e^{-i\phi} e^{i(k_1 z - \omega t)}. \tag{61}$$

The peak voltage difference between the opposing currents is therefore,

$$V = 2 \int_0^a |E_r| \, dr \approx \frac{4\pi}{c} C D I = Z_0 I, \tag{62}$$

where,

$$Z_0 \approx 377 \, CD \, \Omega. \tag{63}$$

When $\theta = 45^\circ$,

$$D \approx \frac{0.55 \cdot 0.6}{(1.2 - 0.44) \cdot 0.6 + 0.55 \cdot (0.4 + 0.6)} = 0.35, \tag{64}$$

so that,

$$Z_0(\theta = 45^\circ) \approx 377 \cdot 1.4 \cdot 0.35 = 185 \, \Omega. \tag{65}$$

In practice, the wires of the twisted pair are insulated, which reduces the characteristic impedance to $\approx 100 \, \Omega$.

For gentle twists ($k_p a \ll 1$) eq. (59) simplifies to,

$$D \approx \frac{I_1(k_p a)}{k_p a I_0(k_p a)} \approx \frac{1}{2} , \tag{66}$$

so that, recalling eq. (50),

$$Z_0(\theta \approx 0) \approx \frac{189}{\sqrt{\cos\theta}} \, \Omega, \tag{67}$$

little different from the value at $\theta = 45^\circ$.

2.4 Energy Flux, Momentum and Angular Momentum Density

At low frequencies where $k_1' \approx k_1 \approx k_p \gg k_f$ the electromagnetic fields for $r < a$ follow from eq. (35)-(40) using eqs. (58) and (60) for the constants E_1 and B_1 in terms of the peak current I,

$$E_r \approx -\frac{4\pi}{c}\frac{CDI}{2}\frac{I_1'(k_p r)}{I_1(k_p a)}\,e^{-i\phi}\,e^{i(k_p z-\omega t)}, \tag{68}$$

$$E_\phi \approx \frac{4\pi}{c}\frac{iCDI}{2r}\frac{I_1(k_p r)}{I_1(k_p a)}\,e^{-i\phi}\,e^{i(k_p z-\omega t)}, \tag{69}$$

$$E_z \approx -\frac{4\pi}{c}\frac{ik_pCDI}{2}\frac{I_1(k_p r)}{I_1(k_p a)}\,e^{-i\phi}\,e^{i(k_p z-\omega t)}, \tag{70}$$

$$B_r \approx -\frac{4\pi}{c}\frac{iC^2DI}{2a}\frac{I_1'(k_p r)}{I_1'(k_p a)}\,e^{-i\phi}\,e^{i(k_p z-\omega t)}, \tag{71}$$

$$B_\phi \approx -\frac{4\pi}{c}\frac{C^2DI}{2ar}\frac{I_1(k_p r)}{I_1'(k_p a)}\,e^{-i\phi}\,e^{i(k_p z-\omega t)}, \tag{72}$$

$$B_z \approx \frac{4\pi}{c}\frac{k_pC^2DI}{2a}\frac{I_1(k_p r)}{I_1'(k_p a)}\,e^{-i\phi}\,e^{i(k_p z-\omega t)}, \tag{73}$$

and for $r > a$ we have the forms (68)-(73) with the substitution $I_1 \to K_1$.

The electric field components (68)-(70) have similar strength (in Gaussian units) to the magnetic field components (71)-(73). The latter correspond to the $m = 1$ term in the series expansions for the quasistatic magnetic fields given in [5]-[8].

The time-average Poynting vector $\langle\mathbf{S}\rangle$ for $r < a$ at low frequencies is,

$$\begin{aligned}\langle\mathbf{S}\rangle &= \frac{c}{8\pi}Re(\mathbf{E}\times\mathbf{B}^\star) = \frac{c}{8\pi}Re[(E_\phi B_z^\star - E_z B_\phi^\star)\,\hat{\mathbf{r}} + (E_z B_r^\star - E_r B_z^\star)\,\hat{\boldsymbol{\phi}} + (E_r B_\phi^\star - E_\phi B_r^\star)\,\hat{\mathbf{z}}]\\ &\approx \frac{4\pi}{c}\frac{C^3D^2I^2}{4a}\frac{I_1(k_p r)I_1'(k_p r)}{I_1(k_p a)I_1'(k_p a)}\left[k_p\,\hat{\boldsymbol{\phi}} + \frac{\hat{\mathbf{z}}}{r}\right],\end{aligned} \tag{74}$$

and that for $r > a$ is obtained from eq. (74) with the substitution $I_1 \to K_1$.

At low frequencies there is no time-average flow of energy in the radial direction, and hence no radiation is emitted by the transmission line.[8]

The energy-flow/Poynting vector (74) is in the same direction as the group velocity (53), as generally expected.[9] Lines of the Poynting flux $\langle\mathbf{S}\rangle$ on the cylinder of radius r follow helices that make angle,

$$\theta_g \approx \tan^{-1} k_p r \tag{54}$$

to the z-axis, such that only at $r = a$ does the energy flow in a helix whose angle matches that of the windings, θ. At small r the (small) energy flows largely parallel to the axis. At large r the angle θ_S approaches 90° and the Poynting vector is almost entirely transverse; however because $K_1(k_p r) \to 0$ at large r there is very little energy associated with these very tight spirals.

[8]Even if we keep the smaller terms in E_ϕ and B_ϕ of eqs. (36) and (39) there is still no radiation emitted by the transmission line at low frequencies.

[9]See, for example, sec. 2.1 of [15] and references therein.

The Poynting vector is at right angles to the wave vector (9), whose angle θ_k to the z-axis is given by eq. (12).

The Poynting vector plays the dual role of describing energy flux and momentum density, where the latter is given by,

$$\langle \mathbf{p} \rangle = \frac{\langle \mathbf{S} \rangle}{c^2} \tag{75}$$

in vacuum. The density $\mathbf{l}$ of angular momentum in the electromagnetic field is therefore,

$$\langle \mathbf{l} \rangle = \mathbf{r} \times \langle \mathbf{p} \rangle = \mathbf{r} \times \frac{\langle \mathbf{S} \rangle}{c^2} \, . \tag{76}$$

On averaging over azimuth ϕ only the z-component of the angular momentum is nonzero,

$$\langle \mathbf{l} \rangle = \frac{4\pi}{c} \frac{C^3 D^2 I^2}{4a} \frac{I_1(k_p r) I_1'(k_p r)}{I_1(k_p a) I_1'(k_p a)} \frac{k_p r}{c^2} \, \hat{\mathbf{z}}. \tag{77}$$

Thus, the electromagnetic waves on a right-handed twisted-pair transmission line carry positive angular momentum. *In a quantum view, the photons of the wave have angular momentum $\hbar$ and energy $\hbar\omega$. Hence, we expect that $\langle \mathbf{l} \rangle = (\langle u \rangle / \omega) \, \hat{\mathbf{z}}$ where $\langle u \rangle = (|E|^2 + |B|^2)/8\pi$ is the time-average electromagnetic energy density. However, this relation is not self evident given the description of the waves in terms of Bessel functions.*

A Appendix: A Single Wire Helix

We can compare the twisted-pair transmission line to the case of a single helical wire [1, 2] in the "sheath" approximation that the helical current flows at angle ψ uniformly over the entire cylinder $r = a$, such that the current and fields have no azimuthal dependence. Then, instead of eqs. (35)-(40) $r < a$, we now have,

$$E_r = -\frac{ik_1}{{k_0'}^2} E_0 \frac{I_0'(k_0' r)}{I_0(k_0' a)} e^{i(k_0 z - \omega t)}, \tag{78}$$

$$E_\phi = \frac{ik_f}{{k_0'}^2} B_0 \frac{I_0'(k_0' r)}{I_0'(k_0' a)} e^{i(k_0 z - \omega t)}, \tag{79}$$

$$E_z = E_0 \frac{I_0(k_0' r)}{I_0(k_0' a)} e^{i(k_0 z - \omega t)}, \tag{80}$$

$$B_r = -\frac{ik_1}{{k_1'}^2} B_0 \frac{I_0'(k_0' r)}{I_0'(k_0' a)} e^{i(k_0 z - \omega t)}, \tag{81}$$

$$B_\phi = -\frac{ik_f}{{k_1'}^2} E_0 \frac{I_0'(k_0' r)}{I_0(k_0' a)} e^{i(k_0 z - \omega t)}, \tag{82}$$

$$B_z = B_0 \frac{I_0(k_0' r)}{I_0'(k_0' a)} e^{i(k_0 z - \omega t)}, \tag{83}$$

and for $r > a$ we have the forms (78)-(83) with the substitution $I_0 \to K_0$.

The condition (41) now implies that,

$${k_0'}^2 E_0 + ik_f \cot\psi B_0 = 0. \tag{84}$$

Similarly, the condition (43) implies that,

$$ik_f \cot\psi\, I_0'(k_0'a)K_0'(k_0'a)E_0 + {k_0'}^2 I_0(k_0'a)K_0(k_0'a)B_0 = 0. \tag{85}$$

The vanishing of the determinant of the coefficient matrix tells us that,

$${k_0'}^4 = -k_f^2 \cot^2\psi\, \frac{I_0'(k_0'a)K_0'(k_0'a)}{I_0(k_0'a)K_0(k_0'a)} = {k_0'}^2 k_f^2 \cot^2\psi\, \frac{I_1(k_0'a)K_1(k_0'a)}{I_0(k_0'a)K_0(k_0'a)}\,, \tag{86}$$

recalling eqs. (33)-(34). That is,

$$k_0' \sqrt{\frac{I_0(k_0'a)K_0(k_0'a)}{I_1(k_0'a)K_1(k_0'a)}} = k_f \cot\psi. \tag{87}$$

At low frequencies such that $k_f a \ll 1$ the factor involving Bessel functions in eq. (87) becomes large, and $k_0' \ll k_f$, as illustrated in the figure below, from [1].

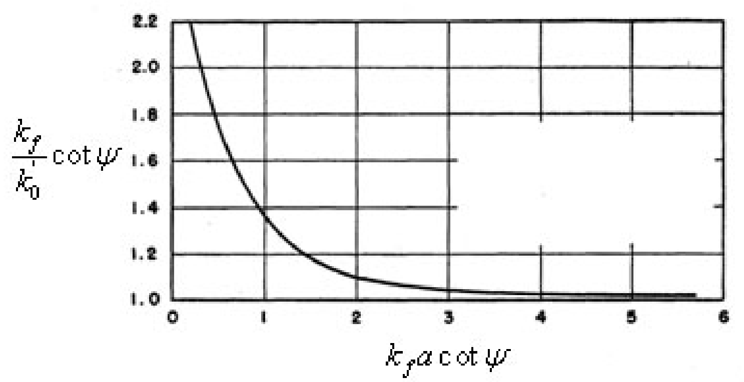

Then, $k_0 = \sqrt{k_f^2 + {k_0'}^2} \approx k_f$ so that the phase velocity and group velocity are both very close to c.

References

[1] J.R. Pierce, *Theory of the Beam-Type Traveling-Wave Tube*, Proc. IRE **35**, 111 (1947), http://kirkmcd.princeton.edu/examples/EM/pierce_pire_35_111_47.pdf

[2] L.J. Chu and J.D. Jackson, *Field Theory of Traveling-Wave Tubes*, Proc. IRE **36**, 853 (1948), http://kirkmcd.princeton.edu/examples/EM/chu_pire_36_853_48.pdf

[3] S. Sensiper, *Electromagnetic Wave Propagation on Helical Structures*, Proc. I.R.E. **43**, 149 (1955), http://kirkmcd.princeton.edu/examples/EM/sensiper_pire_43_149_55.pdf

[4] M. Chodorow and E.L. Chu, *Cross-Wound Twin Helices for Traveling-Wave Tubes*, J. Appl. Phys. **26**, 33 (1955), http://kirkmcd.princeton.edu/examples/EM/chodorow_jap_26_33_55.pdf

[5] H. Buchholtz, *Electrische und magnetische Potentialfelder* (Springer, 1957), p. 292, http://kirkmcd.princeton.edu/examples/EM/bucholz_57.pdf

[6] A.Y. Alksne, *Magnetic Fields Near Twisted Wires*, IEEE Trans. Space Elec. Tel. **11**, 154 (1964), http://kirkmcd.princeton.edu/examples/EM/alksne_ieeetset_11_154_64.pdf

[7] J.R. Moser and R.F. Spencer, Jr, *Predicting the Magnetic Fields from a Twister-Pair Cable*, IEEE Trans. Elec. Compat. **10**, 324 (1968), http://kirkmcd.princeton.edu/examples/EM/moser_ieeetec_10_324_68.pdf

[8] S. Shenfeld, *Magnetic Fields of Twisted-Wire Pairs*, IEEE Trans. Elec. Compat. **11**, 164 (1969), http://kirkmcd.princeton.edu/examples/EM/shenfeld_ieeetec_11_164_69.pdf

[9] D.F. Alferov *et al.*, *The Ondulator as a Source of Electromagnetic Radiation*, Part. Accel. **9**, 223 (1979), http://kirkmcd.princeton.edu/examples/accel/alferov_pa_9_223_79.pdf

[10] P.M. Morse and H. Feshbach, *Methods of Mathematical Physics*, Part 1 (McGraw-Hill, 1953), http://kirkmcd.princeton.edu/examples/EM/morse_feshbach_v1.pdf

[11] V. Onoochin and K.T. McDonald, $\boldsymbol{\nabla} \times (\boldsymbol{\nabla} \times \mathbf{E})$ *in Spherical Coordinates* (Dec. 21, 2020), http://kirkmcd.princeton.edu/examples/curlcurl.pdf

[12] K.T. McDonald, *Bessel Beams* (Jan. 17, 2000), http://kirkmcd.princeton.edu/examples/bessel.pdf

[13] R. Warnecke and P. Guenard, *Some Recent Work in France on New Types of Valves for the Highest Radio Frequencies*, Proc. IEE **100**, 351 (1953), http://kirkmcd.princeton.edu/examples/EM/warnecke_piee_100_351_53.pdf
R. Warnecke *et al.*, *The "M"-Type Carcinotron Tube*, Proc. IRE **43**, 413 (1955), http://kirkmcd.princeton.edu/examples/EM/warnecke_pire_43_413_55.pdf

[14] M. Abramowitz and I.A. Stegun, *Handbook of Mathematical Functions* (Wiley, 1984), http://kirkmcd.princeton.edu/examples/EM/abramowitz_and_stegun.pdf

[15] K.T. McDonald, *Flow of Energy from a Localized Source in a Uniform Anisotropic Medium* (Dec. 8, 2007), http://kirkmcd.princeton.edu/examples/biaxial.pdf

[16] J.A. Stratton, *Electromagnetic Theory* (McGraw-Hill, 1941), http://kirkmcd.princeton.edu/examples/EM/stratton_electromagnetic_theory.pdf